

UNCLASSIFIED

DECLASSIFIED N R L REPORT R-3112

~~COPY NO. 15~~

# K-BAND HARP

DECLASSIFIED by NRL Contract  
Declassification Report  
Date: 14 DEC 2012  
Reviewer's name: H. Do, P. HANNA

Declassification authority: NAVY DECLASS  
GUIDE/NAVY DECLASS MANUAL, 11 DEC 2012,  
03 SERIES



DISTRIBUTION STATEMENT A APPLIES  
Further distribution controlled by UNLIMITED only.

Transmission by Registered Guard Mail  
or U.S. registered mail is authorized  
in accordance with Article 76 (9) of  
the U.S. Navy Regulations.

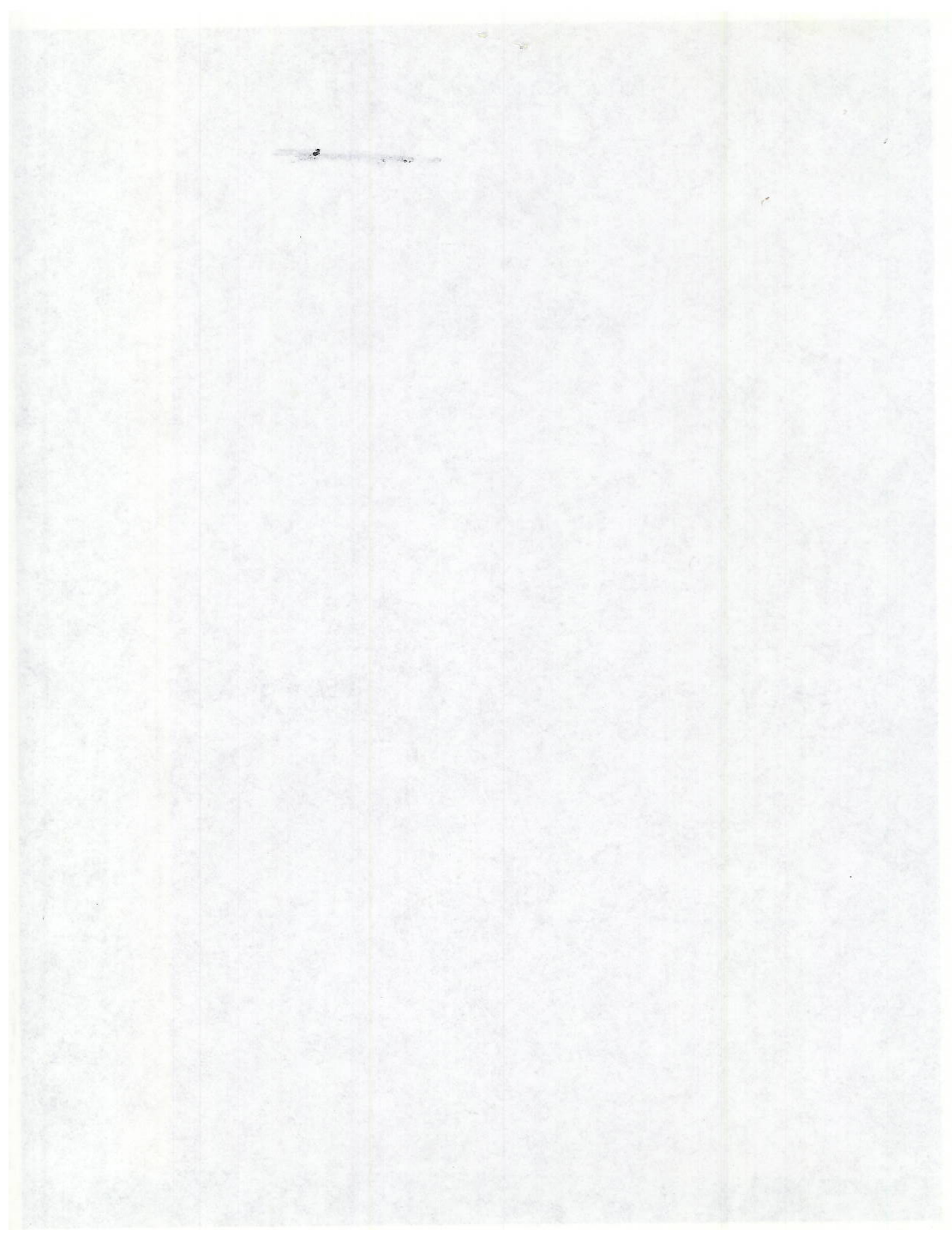


LIBRARY  
NAVAL RESEARCH LABORATORY

NAVAL RESEARCH LABORATORY

Washington, D.C.

DECLASSIFIED



~~SECRET~~  
DECLASSIFIED

DECLASSIFIED

N R L REPORT R-3112

# K-BAND HARP

by

R. W. Wright, M. H. Johnson  
and  
H. A. Tanner

July 1947

Problem No. 34R29-01

Approved by:

J. M. Miller, Superintendent  
Radio Division I

P. Borgstrom, Superintendent  
Chemistry Division

Commodore H. A. Schade, USN  
Director, Naval Research Laboratory



DECLASSIFIED

**NAVAL RESEARCH LABORATORY**

*Washington, D.C.*



DECLASSIFIED

DISTRIBUTION

	Copy Number
ONR	
Attn: Technical Information Section	2-5
BuAer	
Attn: Aer-EL-84	6-10
Attn: TD-4	11
CNO	
Attn: Op-34D	12
Attn: Op-34J	13
Attn: Op-413-B2	14
Attn: Op-413-C6	15
Attn: Op-413-C3	16
CNO NavComAnnex, Wash., D. C.	17
BuShips	
Attn: Code 920	18
Attn: Code 910	19
ComOpDevFor, Norfolk	20
USNEL	21
CO, ONR, Boston	22
OcSigO	23
SNLO, USNEL, Fort Monmouth	24
Dir., ESL, Belmar, N. J.	25
CO, AAF, Wash., D. C.	
Attn: Miss L. Diamond	26
AAF, AMC, LO, BuAer, Navy Dept., Wash., D. C.	27-29
BAGR, CD, Wright Field	30-31
CG, Hdqtrs, AMC, Wright Field	32
CO, AMSC, Watson Labs	33-35

DECLASSIFIED

~~SECRET~~

DECLASSIFIED

DISTRIBUTION (Cont.)

CO, Fort Monmouth Hdqtrs., Bradley Beach	36
CG, SAC, Andrews Field, Wash., D. C. Attn: Operations Analysis Section	37
ComSubFor, Atlantic Fleet, New London	38
NRL Field Station, Boston	39
JRDB	
Attn: Library	40-41
Attn: Navy Secretary	42
NRL:	
Army Liaison Officer (Sig. Corps)	43
Army Liaison Officer (A.A.F.)	44
Code 810	45-46
Code 1340	47-56
Code 186	57-58
Code 187	1
Code 187-A	59-75

DECLASSIFIED

CONTENTS

	Page
Abstract	vi
Introduction	1
Theoretical Results Applicable to Test Procedure	1
K-Band Composition	10
Permeability of K-Band Samples	11
Temperature Variation	12

DECLASSIFIED

ABSTRACT

The properties of Harp materials fabricated from graphite and iron oxide have been studied in the wavelength region 1.1 cm to 1.6 cm. A method of analysis and its application to numerous samples are described in detail. A satisfactory formulation of K-band Harp has been found, and its absorption characteristics studied including its temperature dependence. It is shown that the iron oxide compositions have a small magnetic permeability (1.1) at X-band which disappears at K-band.

DECLASSIFIED

## K-BAND HARP

## I. INTRODUCTION

1.1. Absorbent materials (Harp) have been used to advantage in the S- and X-bands. As K-bands equipment became available, it was evident that Harp could also be applied at this shorter wavelength. Consequently, the development of K-band Harp was initiated at the Naval Research Laboratory under Problem N-41R-S.

1.2. The formulation studies leading to a suitable composition for K-band Harp are described in NRL Report P-2979,\* while the details of the fabricating process are contained in NRL Report P-2987,\*\* both of which reports were issued by the Chemistry Division. The present report deals with the electromagnetic properties of this material, including variations with temperature. A summary of results for experimental lots of material fabricated at various points in the K-band by the above mentioned process is also included.

1.3. The methods of testing K-band Harp are identical with those used at X- and S-band. A brief summary of theoretical results applicable to test procedure is included herein. This work which was done at the Radiation Laboratory, MIT, under the direction of O. Halpern, has not been previously reported.

## II. THEORETICAL RESULTS APPLICABLE TO TEST PROCEDURE

2.1. Propagation in a dielectric medium can be characterized by two constants, the refractive index,  $n$ , and the absorption index,  $k$ . The first constant determines the wavelength in the medium, i.e.

$$\lambda' = \frac{\lambda}{n} \quad (1)$$

where  $\lambda'$  is the wavelength in the medium and  $\lambda$  is the vacuum wavelength. The second constant determines the attenuation of a plane wave in the medium, i.e.

$$k = \frac{\lambda}{2\pi x_0} \quad (2)$$

where  $x_0$  is the distance in which the amplitude of the wave diminishes by the factor  $e^{-1} = 0.368$ .

2.2. Two other constants, the real and imaginary parts of the dielectric constant,  $\epsilon_r$  and  $\epsilon_i$ , are also useful in describing the propagation. The first is connected with

---

\* H. A. Tanner, NRL Report 2979, K-Band Harp Material Formula Development, October 1946. (Secret).

\*\* H. A. Tanner and E. L. Jones, NRL Report 2987, Manufacture of Harp Film by the Spraying Method, October 1946. (Secret).

DECLASSIFIED

$k$  and  $n$  by the relation

$$\epsilon_r = n^2 - k^2 \quad (3)$$

while the second is related to  $k$  and  $n$  by

$$\epsilon_i = 2kn \quad (4)$$

For all cases of interest in this report,  $k^2$  in Eq. (3) can be neglected without introducing appreciable errors. If the loss in the medium arises from a bulk electrical conductivity,  $\sigma$ , then  $\epsilon_i$  is given by\*

$$\epsilon_i = \frac{2\sigma}{\nu}$$

where  $\nu$  is the frequency of the electromagnetic wave. In Harp materials the d-c conductivity is substantially zero. The loss arises from dissipation in the dielectric binder and eddy currents in the conducting particles with which the binder is pigmented.

2.3. An absorbing unit may be constructed by backing a dielectric layer with a metallic reflector. Two conditions must be realized for the complete absorption of an electromagnetic wave incident normally on the dielectric surface. The first is the familiar fact that the thickness,  $d$ , of the dielectric must be a quarter wavelength

$$d = \frac{\lambda'}{4} = \frac{\lambda}{4n} \quad (5)$$

The second is the condition that the loss have the value

$$k = \frac{2}{\pi} \quad (6)$$

When Eq. (6) is satisfied, the absorber is said to be matched. Absorption will also take place if the layer is an odd multiple of a quarter wavelength and will then be complete if  $k$  has the value of Eq. (6) divided by the number of quarter wavelengths in the layer. These relations are valid for  $k^2 \ll n^2$  i.e., when  $k$  is negligible in Eq. (3).

2.4. If  $\lambda_0$  is the wavelength satisfying Eq. (5) (the resonant absorption wavelength) and the incident radiation is of wavelength  $\lambda_0 + \Delta\lambda$ , the power reflection coefficient,  $R$ , for normal incidence is given by

$$R = \frac{\left(\frac{\pi u}{2}\right)^2}{4 + \left(\frac{\pi v}{2}\right)^2} \quad (7)$$

$$v = \frac{n\Delta\lambda}{\lambda_0}$$

Eq. (7) is plotted as Curve A in Figure 1.

2.5. The bandwidth of an absorber is defined as the wavelength region in which the absorber reflects less than a specified fraction of the incident energy. Unless

\* The Gaussian system of units will be used throughout this report.

DECLASSIFIED

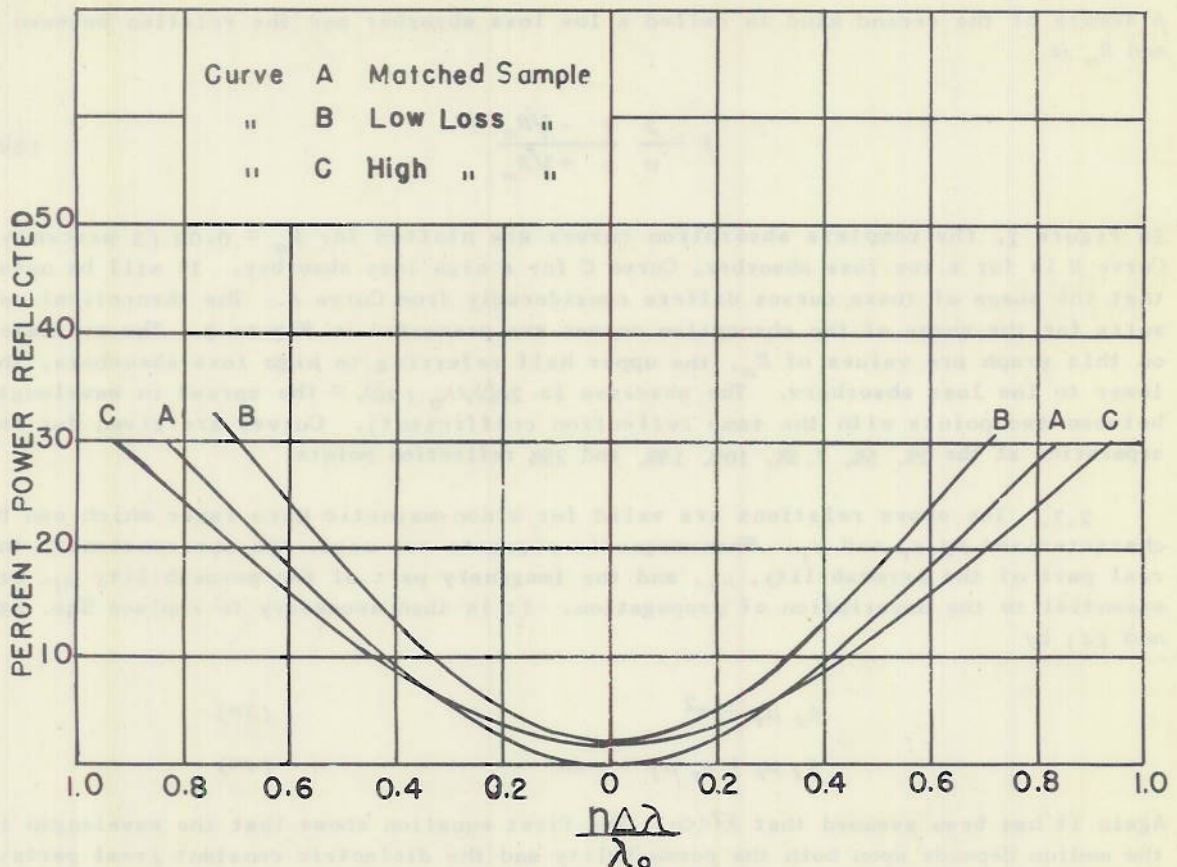


Figure 1. Calculated curves of  $\frac{n\Delta\lambda}{\lambda_0}$  as a function of power reflected for three different type absorbers all at normal incidence.

otherwise stated, this fraction is arbitrarily taken as 5 percent. The statement that the bandwidth of a Harp layer for 1.25 cm is 1 mm means that at least 95 percent of the incident energy is absorbed for any wavelength between 1.20 cm and 1.30 cm. From Eq. (7), the bandwidth of a matched dielectric absorber is

$$\text{bandwidth} = \frac{\lambda_0}{n} \times 0.58 \tag{7a}$$

2.5. Whenever Eq. (6) is not satisfied, the minimum reflection coefficient,  $R_m$ , at the resonant wavelengths, is not zero. A certain value of  $R_m$  then corresponds to two possible values of  $k$ , one larger than that given by Eq. (6), the other smaller. A sample of the first kind is called a high loss absorber and the relation between  $k$  and  $R_m$  is

$$k = \frac{2}{\pi} \frac{1 + \sqrt{R_m}}{1 - \sqrt{R_m}} \tag{8a}$$

A sample of the second kind is called a low loss absorber and the relation between  $k$  and  $R_m$  is

$$k = \frac{2}{\pi} \frac{1 - \sqrt{R_m}}{1 + \sqrt{R_m}} \quad (8b)$$

In Figure 1, the complete absorption curves are plotted for  $R_m = 0.02$  (2 percent). Curve B is for a low loss absorber, Curve C for a high loss absorber. It will be noted that the shape of these curves differs considerably from Curve A. The theoretical results for the shape of the absorption curves are presented in Figure 2. The ordinates on this graph are values of  $R_m$ , the upper half referring to high loss absorbers, the lower to low loss absorbers. The abscissa is  $2n\Delta\lambda/\lambda_0$  ( $2\Delta\lambda$  = the spread in wavelength between two points with the same reflection coefficient). Curves are given for the separation at the 2%, 5%, 7.5%, 10%, 15%, and 25% reflection points.

2.7. The above relations are valid for a non-magnetic Harp layer which can be characterized by  $\epsilon_r$  and  $\epsilon_i$ . When magnetic pigments are used, two new constants, the real part of the permeability,  $\mu_r$ , and the imaginary part of the permeability  $\mu_i$ , are essential to the description of propagation. It is then necessary to replace Eqs. (3) and (4) by

$$\epsilon_r \mu_r = n^2 \quad (3m)$$

$$\epsilon_i \mu_r + \epsilon_r \mu_i = 2kn \quad (4m)$$

Again it has been assumed that  $k^2 \ll n$ . The first equation shows that the wavelength in the medium depends upon both the permeability and the dielectric constant (real parts). The second equation can be rewritten as

$$\frac{k}{n} = \frac{1}{2} \left( \frac{\epsilon_i}{\epsilon_r} + \frac{\mu_i}{\mu_r} \right) \quad (4.1m)$$

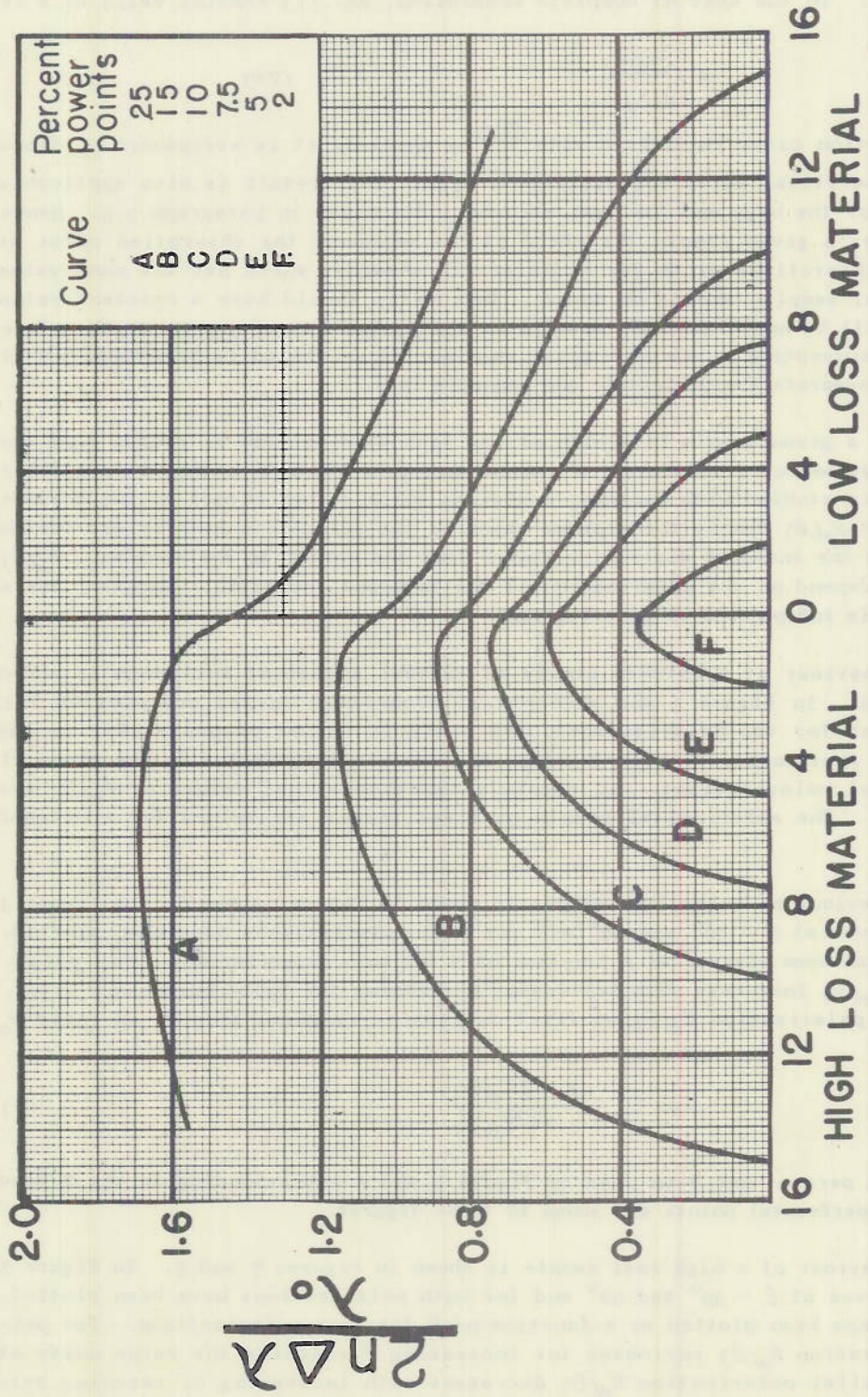
Thus  $k$  is essentially determined by the sum of the phase angles of the dielectric constant and permeability. It turns out in all various experimental arrangements for resonant absorbers so far analyzed that this sum  $\epsilon_i/\epsilon_r + \mu_i/\mu_r$  is the quantity which determines the behaviour of the absorber. Thus for practical purposes these phase angles cannot be separated.

2.8. For magnetic Harp the conditions for complete absorption are

$$d = \frac{\lambda'}{4} = \frac{\lambda}{4n} \quad (5m)$$

$$k = \frac{2\mu_r}{\pi} \quad (6m)$$

It will be noted that the layer must still be a quarter wave thick but that the absorption index must be increased by the factor  $\mu_r$ . The latter fact is an important aid in constructing magnetic absorbers in as much as the phase angle of the permeability is usually large at high frequencies.



### $R_m$ , PERCENT POWER

Figure 2. Calculated curves of  $\frac{2n\Delta\lambda}{\lambda_0}$  as a function of minimum reflection coefficient,  $R_m$ .

2.9. The shape of the absorption curve is altered in a very simple way when the medium is magnetic. In the case of complete absorption, Eq. (7) remains valid if  $u$  is replaced by

$$u = \frac{n\Delta\lambda}{\mu_r\lambda_0} \quad (7m)$$

Thus if the absorption curve is plotted with  $\frac{n\Delta\lambda}{\lambda_0}$  as abscissa it is everywhere  $\mu_r$  times as wide as the theoretical curve for dielectric Harp. This result is also applicable to the discussion of the high and low loss absorbers discussed in paragraph 2.6. Hence to determine  $\mu_r$  for a given sample the ratio of the width of the absorption curve at any point to the theoretical width for a dielectric absorber which has the same value of  $R_m$  as the actual sample, should be found. This ratio should have a constant value equal to  $\mu_r$ . It will be noted that the quantities  $\epsilon_r$ ,  $\mu_r$  and  $\epsilon_i/\epsilon_r + \mu_i/\mu_r$  can therefore be found from the absorption curve of a given sample. As mentioned in paragraph 2.7 it is not possible to separate the dielectric and magnetic loss.

2.10. Whether a given sample is a high or low loss absorber can be judged from the shape of the absorption curve. However, a simpler and more accurate method is available if the reflection is studied with incident radiation which is not normal to the surface of the sample. Let  $R_m(\theta)$  denote the minimum value of the reflection coefficient for an absorption curve at the incident angle  $\theta$  (measured from the normal to the sample).  $R_m(\theta)$  will, in general, depend on the polarization of the incident radiation. However, for a matched sample, it is independent of polarization.

2.11. The behaviour of a matched sample at various angles of incidence is shown in Figures 3 and 4. In Figure 3 the theoretical absorption curves are plotted for  $\theta = 30^\circ$  and  $60^\circ$  and for two polarizations, the electric vector perpendicular to the plane of incidence (perpendicular polarization) and the electric vector in the plane of incidence (parallel polarization). In Figure 4 the theoretical values of  $R_m(\theta)$  are plotted against  $\theta$ . The experimental points on these graphs are values for a matched K-band sample.

2.12. The behaviour of a low loss sample is shown in Figures 5 and 6. In Figure 5 the absorption curves at  $\theta = 30^\circ$  and  $60^\circ$  and for both polarizations have been plotted. In Figure 6  $R_m(\theta)$  has been plotted as a function of  $\theta$  for both polarizations. For parallel polarization  $R_m(\theta)$  increases with increasing  $\theta$  reaching the value unity at  $\theta = 90^\circ$ . For perpendicular polarization  $R_m(\theta)$  at first decreases, reaching zero at an angle  $\theta_0$  given by

$$\cos \theta_0 = \frac{1 - \sqrt{R_m(0)}}{1 + \sqrt{R_m(0)}} \quad (9)$$

A value  $R_m(0) = 18$  percent has been used in Figure 5 and 6 corresponding to the K-band sample for which experimental points are shown in these figures.

2.13. The behaviour of a high loss sample is shown in Figures 7 and 8. In Figure 7 the absorption curves at  $\theta = 30^\circ$  and  $60^\circ$  and for both polarizations have been plotted. In Figure 8  $R_m(\theta)$  has been plotted as a function of  $\theta$  for both polarizations. For perpendicular polarization  $R_m(\theta)$  increases for increasing  $\theta$  reaching the value unity at  $\theta = 90^\circ$ . For parallel polarization  $R_m(\theta)$  decreases with increasing  $\theta$ , reaching zero at an angle  $\theta$  given by Eq. (9). A value  $R_m(0) = 3$  percent has been used in Figures 7

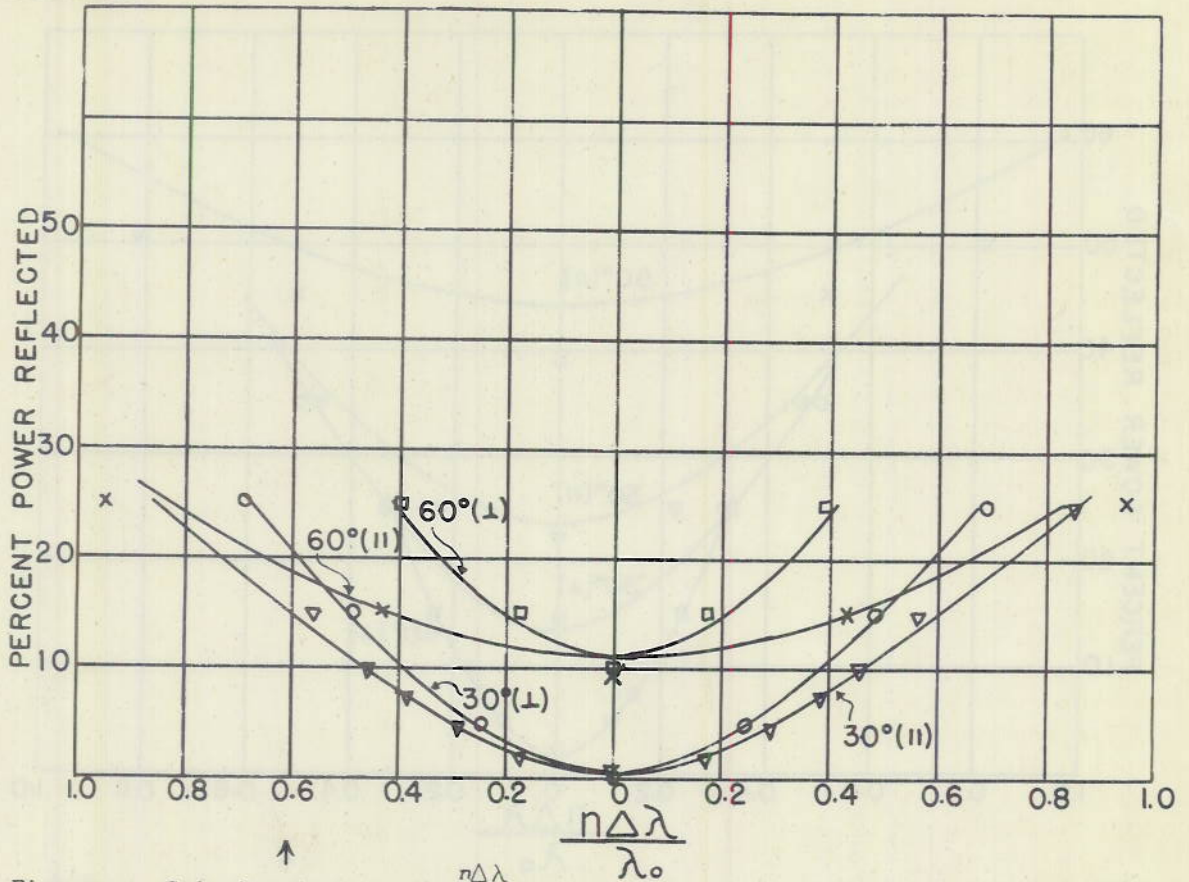
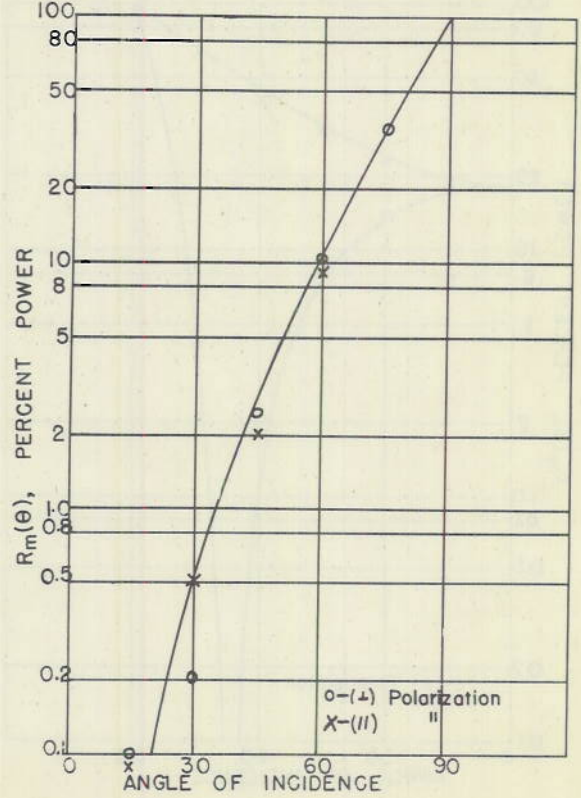


Figure 3. Calculated curves of  $\frac{n\Delta\lambda}{\lambda_0}$  as a function of power reflected, for a material with  $R_m(0) = 0$ , at  $30^\circ$  and  $50^\circ$  angles of incidence for perpendicular and parallel polarizations. The points are experimental data from sample #5107.

Figure 4. Calculated curve of minimum reflection coefficient,  $R_m(\theta)$ , as a function of angle of incidence for a material with  $R_m(0) = 0$ . The points are experimental data from sample #5107.



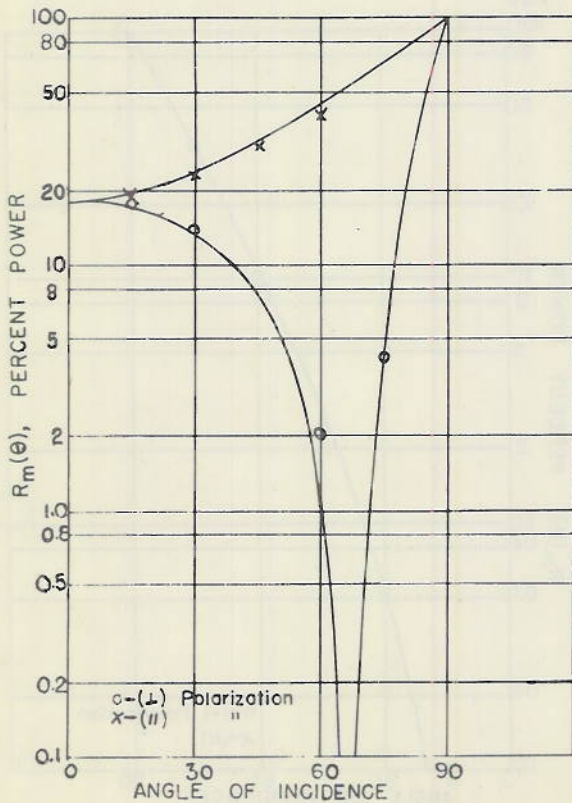
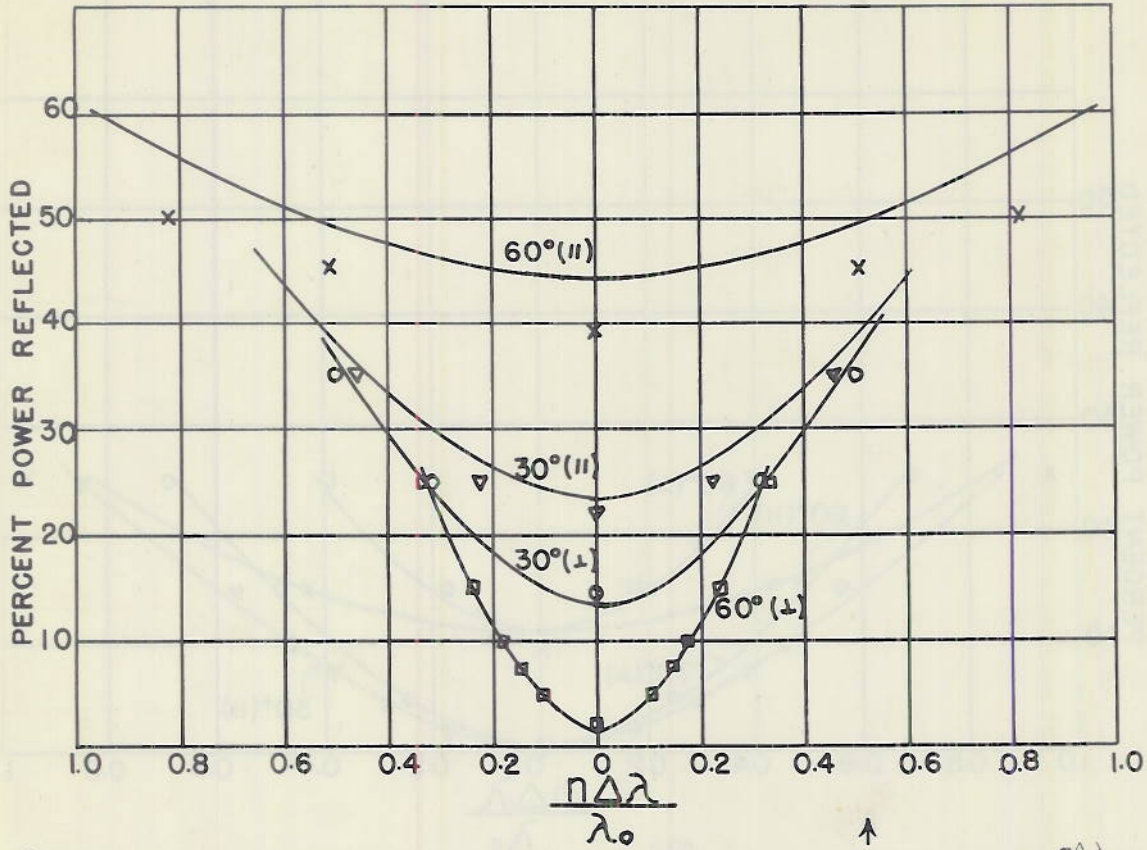


Figure 5. Calculated curves of  $\frac{n\Delta\lambda}{\lambda_0}$  as a function of power reflected, for a low loss material with  $R_m(0) = 18$ , at  $30^\circ$  and  $60^\circ$  angles of incidence for perpendicular and parallel polarizations. The points are experimental data from sample #5088.

Figure 6. Calculated curves of minimum reflection coefficient,  $R_m(\theta)$ , as a function of angle of incidence for a low loss material with  $R_m(0) = 18$ . The points are experimental data from sample #5088.

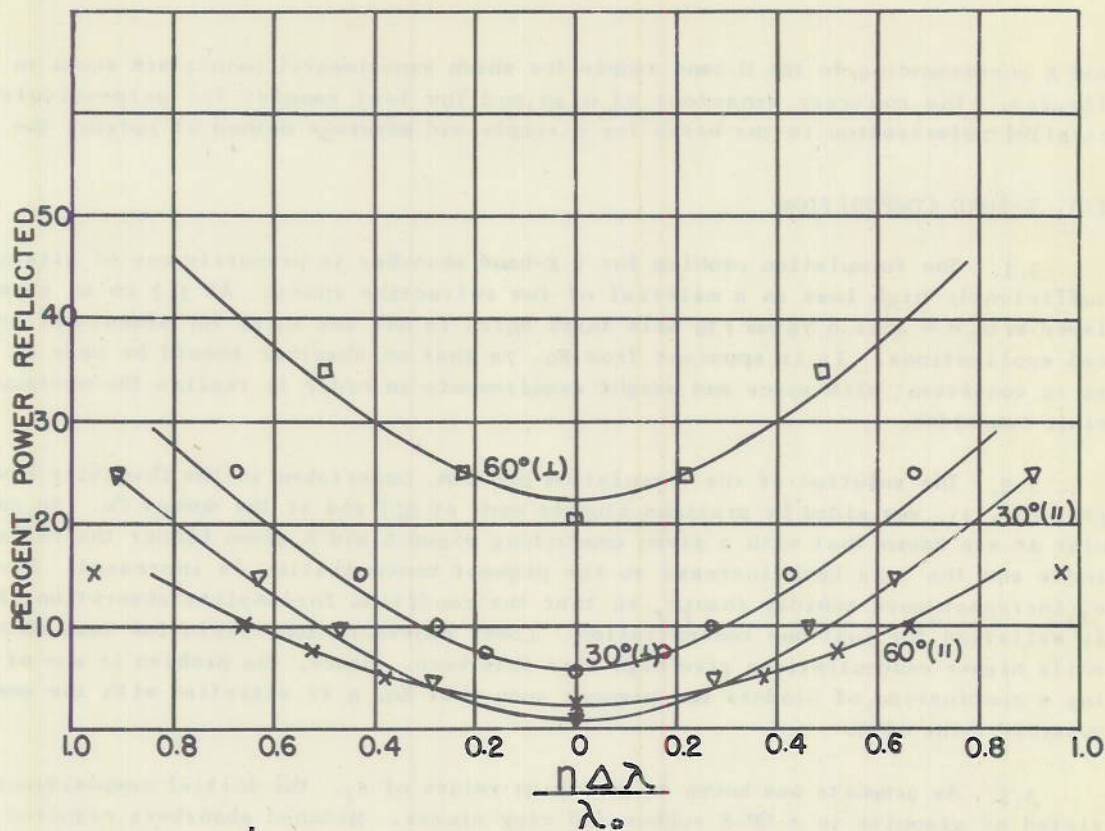
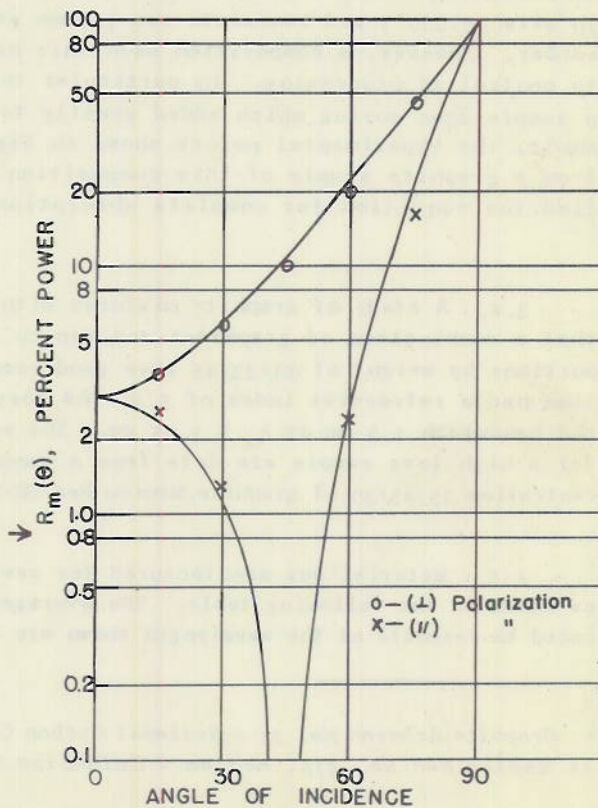


Figure 7. Calculated curves of  $\frac{n\Delta\lambda}{\lambda_0}$  as a function of power reflected, for a high loss material with  $R_m(0) = 3$ , at  $30^\circ$  and  $60^\circ$  angles of incidence for perpendicular and parallel polarizations. The points are experimental data from sample #5252.

Figure 8. Calculated curves of minimum reflection coefficient  $R_m(\theta)$ , as a function of angle of incidence for a high loss material with  $R_m(0) = 3$ . The points are experimental data from sample #5252.



and 8 corresponding to the K-band sample for which experimental points are shown in these figures. The contrary behaviour of high and low loss samples for perpendicular and parallel polarization is the basis for a simple and accurate method of judging the loss.

### III. K-BAND COMPOSITION

3.1. The formulation problem for a K-band absorber is primarily one of attaining a sufficiently high loss in a material of low refractive index. At 1.2 cm an absorbing layer with  $n = 4$  is 0.75 mm (30 mils thick which is not too thick for almost all practical applications. It is apparent from Eq. 7a that an absorber should be made as thick as is consistent with space and weight requirements in order to realize the maximum possible bandwidth.

3.2. The solution of the formulation problem, undertaken in the Chemistry Division (cf. ref. 1), was aided by previous studies made at MIT and at the duPont Co. In particular it was known that with a given conducting pigment and a given binder the refractive index and the loss both increase as the pigment concentration is increased. However,  $\epsilon_i$  increases more rapidly than  $\sqrt{\epsilon_r}$  so that the condition for complete absorption, Eq. 6, is satisfied for just one concentration. Lower concentrations yield low loss absorbers while higher concentrations give high loss absorbers. Hence, the problem is one of finding a combination of binders and pigment such that Eq. 6 is satisfied with the smallest possible value of  $n$ .

3.3. As graphite was known to give high values of  $\epsilon_i$ , the initial compositions consisted of graphite in a GR-S rubber and clay binder. Matched absorbers required about 40 percent graphite concentration and  $n$  was about 6. The corresponding thickness was 20 mils (0.020") and bandwidth was 1.2 mm at  $\lambda_0 = 1.25$  cm. This is a satisfactory absorber. However, a composition with this high graphite concentration proved difficult to control in processing. In particular there were large changes in the loss of such a sample upon curing which added greatly to the difficulty of manufacture. As an example, the experimental points shown in Figs. 5 and 6 for a low loss sample are data from a graphite sample of this composition. Before curing this sample nearly satisfied the condition for complete absorption.

3.4. A study of graphite mixtures with various oxides was then made. It appeared that a combination of graphite\* and Mapico Red\*\* ( $\text{Fe}_2\text{O}_3$ ) in a GR-S binder in the proportions by weight of 33/22/45 gave good results. Matched absorbers with this composition had a refractive index of 5.5, the corresponding thickness being 23 mils (0.023") and bandwidth 1.3 mm at  $\lambda_0 = 1.25$  cm. The experimental points shown in Figures 7 and 8 for a high loss sample are data from a sample made in the Mapico Red series with concentration 25/45/30 of graphite/Mapico Red/GR-S by weight.

3.5. Material was manufactured for several points in the K-band with compositions as shown in the following table. The averaged results for several 2' x 2' samples fabricated to resonate at the wavelength shown are given in this table.

\* Graphite Acheson No. 38 - National Carbon Company.

\*\* Mapico Red No. 516, medium - Columbian Carbon Company.

Resonate Wavelength $\lambda_0$ in CM's	Number of Samples Averaged	COMPOSITION				n	Incident Angles For $R_m \leq 1\%$	Incident Angles For $R_m \leq 5\%$
		Graphite	Mapico Red	GR-S	Neoprene/SRF 4/3			
1.15	10	33	22-1/2	44-1/2	0	5.8	23° to 52° (⊥) 0° to 32° (  ) 0° to 60° (⊥)	
1.25	10	20	20	0	60	5.2	0° to 38° (  ) 0° to 30° (⊥) 0° to 52° (  ) 0° to 48° (⊥)	
1.35	10	33	22-1/2	44-1/2	0	5.7	42° to 50° (⊥) 14° to 57° (⊥)	
1.45	2	20	20	0	60	5.2	0° to 40° (  ) 0° to 27° (⊥) 0° to 55° (  ) 0° to 46° (⊥)	
1.55	10	30	23-1/2	23	23	6.1	0° to 47° (  ) 0° to 8° (⊥) 0° to 48° (  ) 0° to 40° (⊥)	

The experimental points shown in Figures 3 and 4 are data for a sample having one of these compositions. The bandwidths are accurately determined by Eq. 6 as evidenced by the excellent agreement with the theoretical absorption curves in Figure 3.

#### IV. PERMEABILITY OF K-BAND SAMPLES

4.1. Iron oxides were introduced originally in the hope that magnetic loss might still be present at K-band wavelengths and thereby  $k/n$  might be increased (cf. Eq. 4.1 m). However, the agreement between the theoretical absorption curve and the experimental points (Fig. 3) shows that the real part of the permeability does not differ from one by more than 3 percent. Hence it is unlikely that the magnetism is an important factor in the loss, which must therefore be dielectric in origin.

4.2. To examine the magnetic behaviour in more detail, a sample 60 mils (.060") thick was fabricated for test in the X-band. It could then also be tested as a three quarter-wave absorber in the K-band. The experimental results are shown in Figure 9. It will be noted that in the K-band the results are in excellent agreement with the theoretical absorption curve\* for the measured value of  $R_m(30)$  while at X-band the width of the absorption is definitely wider than the theoretical curve. This indicates that  $\mu_r$  is very close to one in the K-band while in the X-band it has a value between 1.1 and 1.2. This conclusion is substantiated by the ratio of the resonant wavelengths at X- and K-band. For according to Eq. 5 and the corresponding equation for a three quarter-wave absorber, the ratio of refractive indices at X- and K-band is equal to 1/3 the ratio of resonant wavelengths. Experimentally the latter quantity is 1.04. If the increase in  $n$  is entirely due to permeability at X-band, Eq. 3 m gives approximately 1.1 for the X-band permeability.

4.3. A further indication of magnetism at X-band which is not present at K-band is given by comparing the loss of the sample in Figure 9. At X-band it is very close to a match. If  $k$  had the same value at K-band, the loss would be three times too great for a three quarter-wave absorber corresponding to a minimum reflection of 25 percent.

\* In computing the theoretical curve for a three quarter-wave absorber, the wavelength spreads for a corresponding quarter-wave absorber must be divided by three. Likewise in determining  $k$  from Eq. 8a or Eq. 8b the right hand member must be multiplied by 1/3.

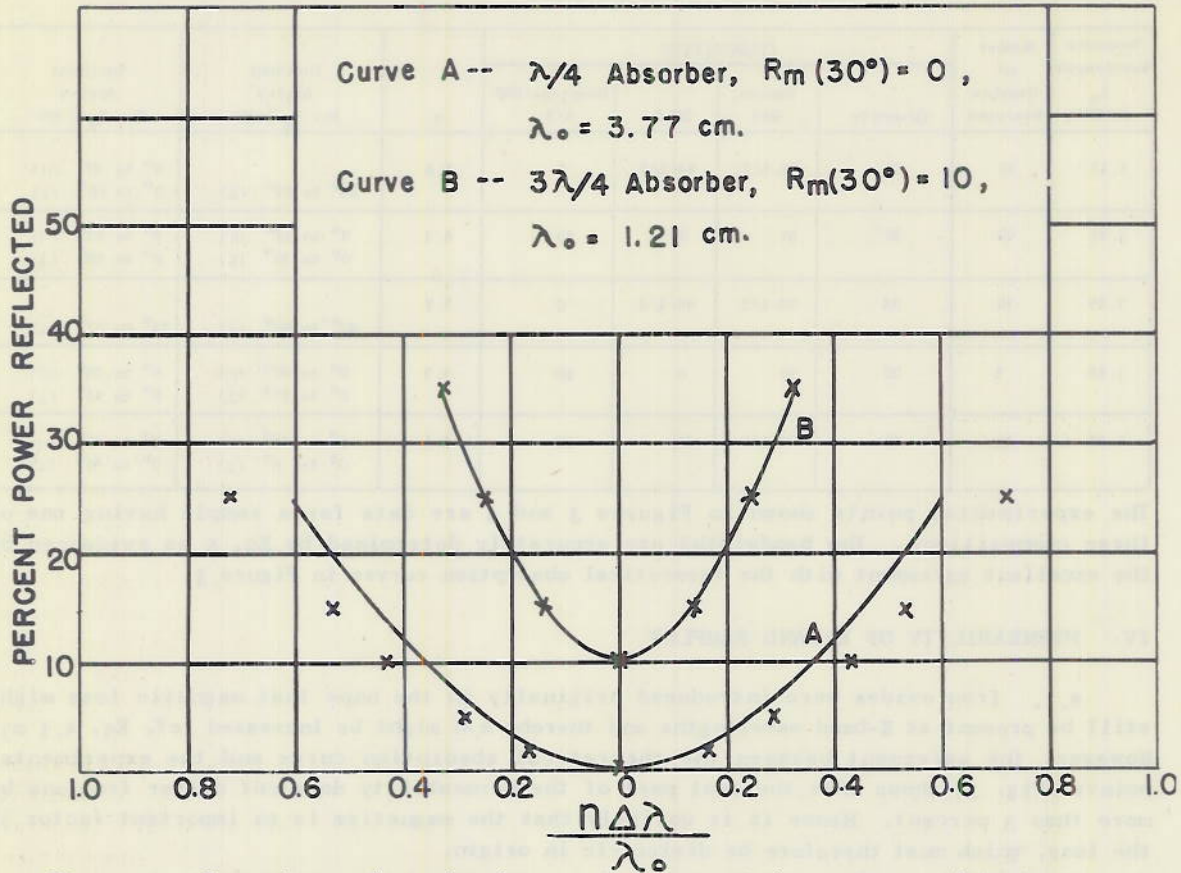


Figure 9. Comparison of an absorber at its  $\lambda/4$  and  $3\lambda/4$  points. Calculated curves of  $\frac{n\Delta\lambda}{\lambda_0}$  as a function of power reflected for  $30^\circ$  angle of incidence and perpendicular polarization. The points are experimental data from sample #5490.

The experimental value is 11 percent corresponding to a loss only twice too great. The added phase angle, Eq. 4.1m, can reasonably be ascribed to an imaginary component of the permeability at X-band which disappears at the shorter wavelength. It is to be expected that at frequencies where  $\mu_r$  is approaching unity, a relatively large imaginary component of the permeability will be present.

V. TEMPERATURE VARIATION

5.1. A limited study has been made of the temperature sensitivity of several K-band compositions. The change in loss with temperature can be immediately deduced from the minimum reflection coefficients. Likewise the shift in resonant frequency with temperature is directly measurable. However, the determinations of refractive index require accurate measurements of small changes with temperature in thickness of the sample and were therefore not undertaken.

5.2. A sample of 40 percent graphite in a clay GR-S binder gave the results shown in the following table.

Sample No. 5111 $\lambda_o = 1.135$ cm. $n = 6$			
Temperature °C	Change in $\lambda_o$ in cm	$R_m(30^\circ)$	$k/k_o$
26.5	0	0.5	1.0
50	-.025	3.0	0.7
75	-.050	6.0	0.6

The shift in resonant wavelength could result from either a lower refractive index or a greater thickness at the elevated temperature ( $\lambda_o = 4nd$ ). The decrease in loss at higher temperatures is due to the peculiar characteristic of graphite that its resistance decreases with increasing temperature.

5.3. A sample of the graphite /iron oxide/ GR-S composition was also studied. Here a shift in wavelength was almost the same as shown in the table. The loss change was similar to that shown in the table except the changes were considerable smaller. The effect of the diminishing resistance in the graphite was smaller because of the lower graphite concentration.

5.4. A sample of the composition for MX410/AP Harp which consists of aluminum flake in an SRF (carbon black) neoprene mixture was also examined. The shift in resonant wavelength was again toward shorter wavelengths but the loss now increased with temperature, from  $k/k_o = 1$  to  $k/k_o = 1.2$ . A similar result had been found for this composition at X-band wavelengths.

5.5. It is evident from these results that the temperature sensitivity of the loss could be greatly reduced, if this should ever prove necessary, by proper mixture of graphite with another conducting flake.

